Marine Pollution Bulletin 165 (2021) 112112

Contents lists available at ScienceDirect

Marine Pollution Bulletin

journal homepage: www.elsevier.com/locate/marpolbul

Impacts of a temperate to tropical voyage on the microalgal hull fouling community of an atypically-operated vessel

Christine A. Edmiston [a,*], William P. Cochlan [a], Christopher E. Ikeda [a], Andrew L. Chang [b]

[a] Estuary & Ocean Science Center, San Francisco State University, Tiburon, CA, USA
[b] Smithsonian Environmental Research Center, Tiburon, CA, USA

ARTICLE INFO

Keywords:
Microalgae
Biofouling
Vessels
Microfouling

ABSTRACT

Microalgal communities that colonize the hulls of at-risk vessels – those which have the highest port residency times, lowest speeds, and most stationary time in water - are expected to change as a function of environmental factors during ocean voyages, but are rarely studied. The microalgal communities on the hull of an atypically operated ship, the T.S. *Golden Bear*, were quantified during the course of a voyage from San Francisco Bay to the South Pacific and back. Here we clearly demonstrate that microalgal communities can be highly resilient, and can survive physiologically strenuous journeys through extreme variation in salinity and temperature. A 42% reduction in microalgal biomass and a 62% reduction in algal cellular abundance indicated a community-wide negative reaction to an increase in both salinity and temperature after the ship left San Francisco Bay, CA and cruised southward to Long Beach, although *in vivo* cellular fluorescence capacity increased. Further reductions in biomass (36%) and cellular abundance (26%) occurred once the ship encountered high-temperature, high-salinity waters in Hawaii. A 17% reduction of cellular fluorescence capacity was also observed in Hawaii. Despite previous environmental stressors, upon return to temperate waters off Vallejo, CA, biomass increased 230%, cellular abundance remained stable, and cellular fluorescence capacity increased from 0.45 ± 0.26 to 0.60 ± 0.07. The methods used in the current research provide efficient, cost-effective procedures for analyzing microalgal (and macrofouling) communities, which can in turn aid regulators in creating such necessary thresholds for enforcement.

1. Introduction

Marine biofouling is a leading vector of marine introduced species on a global scale (eg, Davidson et al., 2014). In California's coastal waters, over 257 non-native species are established, 48% of which can be attributed exclusively to vessel traffic vectors, including hull fouling, ballast water, dry ballast, and cargo (Ruiz et al., 2011). Over half of the non-native species established in California were first recorded within the San Francisco Bay Estuary (SFBE; Ruiz et al., 2011).

Biofouling communities are broadly composed of organisms of two size groups: macrofouling (eg, barnacles, mussels, tunicates, and other larger organisms) and microfouling (eg, microalgae and bacteria) communities (Brandt et al., 2009). The micro- and macroorganisms that make up biofouling communities can cause substantial environmental and ecological damage, and incur significant costs to the maritime shipping industry and its stakeholders. For instance, when fouling organisms attach to the bottom or sides of a ship, they increase drag, which drastically lowers a ship's fuel efficiency. Microfouling (a thin layer of algae, debris, and bacteria) alone can increase fuel consumption by up to 15% and reduce sailing speed by 20% (Lewin, 1984; Schultz et al., 2011; Van Rompay, 2012). Lowered fuel efficiency results in higher exhaust emissions, which are damaging for the environment (Bott, 2009) and lead to greater operating costs for the maritime industry (Schultz et al., 2011).

While there is an abundance of scientific studies on macrofouling and associated environmental risks (eg, Carlton and Hodder, 1995, Gollasch, 2002, Cao et al., 2010; Davidson et al., 2009; Coutts et al., 2010; Williams et al., 2013; Chang et al., 2018), relatively little is known about the biosecurity risks associated with microalgal communities and their transport *via* hull biofouling. To date, there are very few published studies that focus on in-service ships and the impacts of abiotic factors and transit on microalgal species, such as diatoms (Callow, 1986; Woods et al., 1986; Zargiel et al., 2011; Hunsucker et al., 2014; Sweat et al., 2017). Microfouling communities are widely acknowledged to be

* Corresponding author at: Estuary & Ocean Science Center, San Francisco State University, Tiburon, CA, USA.
E-mail address: christineaedmiston@gmail.com (C.A. Edmiston).

https://doi.org/10.1016/j.marpolbul.2021.112112
Received 5 August 2020; Received in revised form 25 January 2021; Accepted 26 January 2021
Available online 9 February 2021
0025-326X/

present and transported worldwide on vessel hulls, and can comprise widely diverse groups (eg, Leary et al., 2014). Yet the paucity of quantitative information on these communities, combined with the well-known risks posed by macrofouling, suggests that biofilms and microalgal fouling communities likely constitute a significant invasion risk.

Several risk factors influence biofouling accumulation across the global fleet, including vessel type, with widely varying operational profiles, characteristics, and behaviors (Davidson et al., 2017). Biofouling accumulation, and thus the risk of transporting non-native species, increases as a ship remains in one location for a prolonged period of time, whether docked at port or at anchor in a harbor (Zargiel and Swain, 2014), but this relationship is generally poorly quantified (Davidson et al., 2020). While most vessels, such as container ships, minimize their time in port, there are other vessels that will remain in port for weeks to months at a time (Inglis et al., 2010; Schimanski et al., 2017). These 'atypically-operating' vessels, by definition, remain in one location for ten or more days before resuming their normal operations and voyages. Such vessels may include, but are not limited to, military ships, floating platforms (barges) and training ships (Davidson et al., 2009). The number of atypically-operating vessels can be significant: in one four-year period from 2011 to 2015, over 7800 vessel arrivals to California waters were reported from origin ports around the world following lay-up periods exceeding ten days and without any biofouling management before arrival (Scianni et al., 2019; Davidson et al., 2020).

The California State Lands Commission's Marine Invasive Species Program is one of the first regulatory agencies in the US to address biofouling as a biosecurity risk, by implementing maritime laws to mitigate the potential risk posed by heavily-fouled ships arriving at California ports (Zabin et al., 2018; Scianni et al., 2019). In order to prioritize limited resources effectively, regulators need a better quantitative understanding of the relative risk of non-native species transport within biofouling communities as a function of vessel type and their operational profile.

The TS *Golden Bear* is the training ship of the California State University Maritime Academy. Although this ship remains in port for eight months of the year, each summer it departs the San Francisco Bay Estuary (SFBE) during an annual training cruise to various global locations. At the time of this study in 2018, the ship's hull had not been cleaned for five years (the maximum allowed for any operational vessel under the International Convention for the Safety of Life at Sea (SOLAS, 2020)). As a result, there was well-established biofouling community for observation during this study as the vessel transited from the estuarine conditions of SFBE to the marine conditions of temperate coastal ports along the California coast, then to tropical ports in the mid-Pacific Ocean. The existing hull fouling community at the beginning of this study was thus comprised of organisms from the SFBE as well as those that may have originated from a range of locations during the vessel's recent training voyages during the past five years to the South Pacific, western and eastern coasts of the United States, U.S. Virgin Islands, Europe and through the Panama Canal. The 2018 route allowed for repeated measurement of the response of the biofouling communities to a gradient of salinity and temperature conditions in transit, and permitted observational analyses of both the microfouling and macrofouling communities.

The current study first characterizes the microalgal organisms that grow on vessels, specifically on those vessels which pose the highest risk of supporting well-developed communities that can be transported elsewhere, such as atypically-operating ships with their high port residency times, low speeds, and long stationary times in water; secondly, it focuses on the poorly-studied microalgal communities which often facilitate the subsequent settlement of larger macrofouling organisms (eg, Wahl, 1989); and thirdly, it confirms whether differences in salinity and transit impact the physiological health of microalgal communities.

Three main objectives are addressed in our study by testing the following hypotheses:

Microalgal biomass on the ship's hull, measured as chlorophyll *a* concentration, is reduced throughout transit as a function of time and environmental changes.

The photosynthetic efficiency of the microalgal community, measured as *in vivo* cellular fluorescence capacity, is reduced during the ship's transit as a function of time and environmental changes.

Both the microalgal cell density and the microalgal community composition is reduced throughout the ship's transit as a function of time and environmental changes.

Additionally, the use of remotely operated vehicles (ROVs) and video footage were examined to determine their effectiveness as a means of observing changes in the biofouling community over a range of environmental conditions and time periods. ROVs are the current, preferred method of observation for the California State Lands Commission when conducting in-water surveys, and thus our study provided an opportunity for both (1) testing the current methods employed and (2) reviewing and providing suggestions for further usage of these units in various locations and conditions within the SFBE.

2. Materials and methods

2.1. Study vessel

The Training Ship *Golden Bear* (Fig. 1) was chosen as the research vessel for this project to evaluate the effects of transit and environmental changes on biofouling communities on a ship's hull. This large vessel (length: 152 m; beam: 22 m; gross tonnage: 12,517 t) was an ideal platform for this research for three reasons: 1) it remains in port for eight months at a time, and thus, by definition, is an atypically-operated vessel; 2) given that it is an educational and training ship, operated by the California State University Maritime Academy, it allows access for researchers - which is rare in the maritime industry; and 3) it travels through a gradient of salinity and temperature conditions during its an annual academic training cruise over a relatively short period of time (<3 months). Here, we assess the biofouling communities on the hull of the T.S. *Golden Bear* during its summer 2018 round-trip voyage from San Francisco Bay to the South Pacific and back.

2.2. ROV video sampling

Transects were run at a depth of approximately 1 m below the surface to capture images and videos of the extent of microalgal and macrofouling communities on the hull of the T.S. *Golden Bear.* Continuous video footage at the forward, mid-ship and aft sections of the hull were taken *via* ROVs (Seabotix LBV200 and LBV200-4) while the ship was either anchored or secured alongside the wharf at four stops during its

Fig. 1. Image of the Training Ship *Golden Bear* showing the three sampling sections of the hull (Photo by Jules Kuo, Hawaii Division of Aquatic Resources). Note: due to inaccessibility issues while docked at ports, only the starboard side was sampled during this study.

summer voyage. The ROV in Vallejo, CA, on April 24th was also equipped with a high-definition video camera (GoPro Hero™ 7; GoPro, Inc., San Mateo, CA, USA). All other sampling locations relied solely on ROV footage, since no GoPro was attached to the ROV. Using a GoPro™ HERO 7 attached to an extension pole also provided an opportunity to collect video data using a low-cost alternative method to an ROV.

Each port had distinctly different environmental conditions, such that the voyage spanned a wide range of ambient salinities and temperatures (Table 1). Images and video from the ROV transects were used to qualitatively assess survivorship and community composition during the voyage to evaluate the impacts of transit and changing environmental conditions on the macrofouling organisms.

2.3. Biological collections and analysis

Biological samples were collected from the hull of the T.S. *Golden Bear* either in port (Vallejo, CA) or out at anchor (Long Beach, CA, and Lahaina, HI). Due to the inability to access the waterline on the port side, only the vessel's starboard side was sampled at the forward, mid-ship, and aft sections (Fig. 1). Due to safety concerns and further sampling feasibility, physical scraping only occurred at the waterline depth.

Prior to removing any biofouling from the vessel, *in situ* environmental conditions were recorded at the surface, and 1 and 2 m depths using a YSI Model probe (YSI Inc., Yellow Springs, Ohio, USA) near the forward, mid-ship, and aft sections of the ship. Discrete water samples were collected from the water immediately adjacent to the three main sections of the hull (hereafter referred to as "pelagic samples") at each port stop to provide quantitative estimates of neighboring pelagic communities in addition to the benthic samples scraped from the hull. Pelagic sampling was done prior to any hull sampling to prevent possible contamination by hull scrapings. Physical hull sampling was conducted by pulling a 6-inch rubber, soft-sided window scraper across the ship's hull within a 1 square meter (1 m^2) quadrat. These samples were immediately placed into plastic bags upon collection, cooled by placing on ice, and stored in darkness to prevent photodegradation. All samples from the hull of the ship and the adjacent water samples were transported to San Francisco State University's Estuary & Ocean Science Center (EOS Center) within 12 h for subsequent analyses or storage.

In the laboratory, hull samples (collected from the field) were transferred into 50-mL polyethylene bottles and brought up to a volume of 10 mL using previously filtered (Whatman™ 25-mm diameter GF/F filters; nominal pore size = 0.7 μm; GE Healthcare Life Sciences, Piscataway, NJ, USA) sea water. Because samples could not be filtered at the time of collection nor frozen until analyses, these samples were then incubated for 48 h under controlled conditions: the incubators employed the *in situ* temperature of collection and were maintained on a 12:12 h, light:dark cycle before all samples were prepared for analyses of algal biomass, photosynthetic efficiency, cellular abundance and species identification.

2.4. Biomass as Chlorophyll *a*

Algal biomass was measured as chlorophyll *a* (Chl *a*) concentration using the *in vitro* acidification method (Parsons et al., 1984), which corrects for pheophytin *a* (Arar and Collins, 1997; Hauer and Lamberti, 2007). Samples from both the pelagic seawater and the algal-seawater hull scraping mixture (described above) were collected by filtering 20 mL of the sample water onto 25-mm diameter Whatman™ glass-fiber filters, which were stored in a freezer at −20 °C until analysis. Pigments collected on the filters were then extracted with 6.5 mL of 90% acetone (HPLC grade, ACROS Organics™, Geel, Belgium) for approximately 24 h in the dark at −20 °C. Samples were then analyzed using a 10-AU fluorometer (Turner Designs, San Jose, CA) calibrated with pure Chl *a* obtained from Turner Designs. In order to prevent any photodegradation, the filtration and pigment analyses were carried out in a low light environment.

2.5. Algal photosynthetic efficiency

In vivo cellular fluorescence capacity (F_v/F_m), is related directly to the maximum photochemical quantum efficiency of Photosystem II (PS II), and was measured here for both pelagic and algal-seawater hull scraping samples with a Turner Designs 10-AU fluorometer, where an electron transport inhibitor was employed to close the PSII reaction centers, and thus maximize fluorescence. The cellular fluorescence capacity, as a proxy for algal photosynthetic efficiency, was determined as the ratio of variable (F_v) to maximum (F_m) fluorescence measured after dark acclimation (10 min) using the 3-[3,4-dichlorophenyl]-1,1-dimethylurea (DCMU) inhibitor technique (Parkhill et al., 2001). Variable fluorescence was calculated using the equation $F_v = F_m - F_o$, where F_o is background fluorescence of the cells (all of the PSII reaction centers are open), and F_m is the "maximal fluorescence" before non-photochemical quenching (eg, xanthophyll cycling) is initiated.

2.6. Microalgal cellular abundance and species identification

The previously diluted samples were inverted three times, and then 1.5 mL of the sample/seawater mixture from each sample was transferred into 1.5-mL microcentrifuge tubes (Fisherbrand™ Premium Microcentrifuge Tubes). Samples were then preserved with the addition of 0.15 mL of Lugol's Iodine solution to a final concentration of 0.1% (v/v). The preserved samples were then thoroughly mixed prior to storage in a refrigerator (8 °C) for future analyses. These preserved samples were then prepared for identification by microscopy by first vortexing at 6000 rpm for 20 s, followed by three inversions. The samples were then cleared of all organic material with a commercial drain cleaner (Drano®, S.C. Johnson & Son, Racine, WI, USA). A permanent slide was prepared by placing the cleaned sample on a glass slide and adding a drop of high refractive index mounting medium. A coverslip was then

Table 1
Environmental conditions for the four dates of sampling: temperature, salinity, pelagic algal cellular abundance, pelagic biomass (as Chl *a*), and algal photosynthetic efficiency (as *in vivo* cellular fluorescence capacity; F_v/F_m) from pelagic water samples collected adjacent to the vessel's hull prior to sampling the hull for benthic scrapings. Means of replicates ($n = 9$) are presented for cellular abundance, biomass, and photosynthetic efficiency. Average speed of the TSGB throughout the summer 2018 voyage is presented in advance knots (kts).

Location	Date	Temp (°C)	Salinity	Pelagic cellular abundance ($\times 10^3$ cells/L)	Pelagic biomass (μg Chl *a*/L)	Pelagic photosynthetic efficiency (F_v/F_m)	Average speed of advance (kts)
Vallejo, CA	4/24/18	16.4	11.5	20.05	2.48	0.53	14.0 ± 2.5
Long Beach, CA	5/01/18	16.1	33.5	2.81	5.42	0.72	
Lahaina, HI	6/14/18	25.6	35.0	0.50	0.03	0.51	
Vallejo, CA	6/29/18	18.9	20.4	60.17	1.16	0.63	

placed over the sample before heating the slide to burn off excess alcohol (Diatom Project, 2010).

2.7. Flow cytometry

Flow cytometry was used to quantify the cell density (BD Accuri C6 flow cytometer; BD Bioscience, San Jose, CA, USA). The preserved 1.5-mL samples were vortexed at 6000 rpm for 20 s, and then inverted three times to ensure a homogeneous mixture of the sample. From these samples, 30-μL sub-samples were analyzed within one minute. Cell size was determined from forward-scattered light (FSC) values, which are proportional to cellular surface area (Shapiro, 2003; Ikeda et al., 2016). The different microalgal species were totaled by selection of the population based on the sizes acquired through microscopy and non-fluorescent particle size calibration beads that ranged in size from 1 to 15 μm in diameter (F-13838; Molecular Probes, Grand Island, NY, USA). The cellular abundance for each population was then calculated using the equation

$$cellular\ abundance = \frac{g}{S} \times 1000$$

where g is the total count obtained from the "gated" region, and 'S' is the volume (μL) subsampled by the flow cytometer (Ikeda et al., 2016).

Eight samples were randomly selected for direct comparison of enumeration conducted by flow cytometry *versus* enumeration by inverted microscopy). Due to over dispersion of the count data, a negative binomial error distribution and log link function were specified (glm.nb function, MASS package) during this statistical analysis Despite the consistently lower counts *via* microscopy, enumeration *via* flow cytometry was directly proportional to measurements of cellular abundance *via* microscopy.

2.8. Statistical analysis

All statistical analyses were conducted in R (Version 3.0.3; R Core Team, 2018) and Rstudio (Version 0.97.551; Rstudio Team (2018)). Generalized linear models (GLM) were used to examine the impact of the voyage on algal biomass (measured as Chl *a*). Due to over dispersion of the biomass data, a negative binomial error distribution and log link function were specified (glm.nb function, MASS package; Venables and Ripley, 2002). Cellular abundance was also examined with a generalized linear model with a negative binomial error distribution and log link function. Algal photosynthetic efficiency was examined using a linear model (lm function, R Core Team, 2018). Nested models were assessed based on the location on ship (forward, mid-ship, aft) and the port location (Vallejo, CA, Long Beach, CA, Lahaina, HI). Then, the best fit model was selected using Akaike Information Criterion (AIC) to compare models, in which the lowest AIC value represents the best fit (Burnham and Anderson, 2004).

3. Results

3.1. Observations of the fouling community at each port

The fouling community of the TS *Golden Bear* was observed at three different ports during its summer 2018 voyage: Vallejo, CA, Long Beach, CA, Lahaina, HI, and again two months later in Vallejo. ROV video footage from Long Beach was compromised and unavailable for comparison, but footage from the other three sampling dates indicated a shift in the macrofouling species attached to the ship's hull.

The first survey was conducted in Vallejo on April 24, 2018. Biofouling growth was observed on all sections of the ship's hull: from the waterline to 1 m depth, at least half of the area was covered in barnacles (*Balanus* spp.), while much of the hull was covered with green microalgae spreading from the waterline to below the ROV's video capacity (3 m depth). In some areas, barnacles were clumped in large vertical bands (Fig. 2). The macroscopic fouling organisms present were primarily filter-feeders, and the introduced isopod, *Synidotea laticauda,* was commonly found among the shells of living and dead barnacles. This first survey of the TS *Golden Bear* showed the extent of biofouling accumulation since its last dry-dock maintenance conducted five years previously.

The second survey, conducted at Long Beach, CA on May 1, 2018 showed little qualitative change in the community compared to the initial survey at Vallejo. While in Long Beach, intermittent bands of barnacles (2-m wide areas with approximately 90–100% coverage of barnacles) were observed to be actively feeding at the waterline and below. The spatial extent and composition of the community resembled that observed at Vallejo: microalgae were present along the waterline and extended below 3-m on the hull along with consistent barnacle coverage.

By the time the ship arrived at Lahaina, HI on June 14, a clear shift was visible in the macrofouling community, with no survivorship observed of the previously dense, actively feeding bands of barnacles observed at Vallejo and Long Beach. Now only hollow shells were visible. Due to good water clarity, the entire starboard side of the ship was readily observable, from the waterline to the bottom of the keel, and 90% of the hull was covered in microalgae and hollow barnacle shells.

3.2. Pelagic water samples

The ambient conditions of the pelagic waters adjacent to the ship demonstrated increased salinity levels expected in coastal and oceanic waters of Long Beach and Lahaina, respectively, relative to estuarine waters of Vallejo (Table 1). Lahaina had the highest temperature and salinity of the four sampling opportunities, and both temperature and salinity increased at Vallejo after two months due to decreased seasonal freshwater flow at the later date. Chlorophyll *a* was initially 2.48 μg/L in the temperate waters of Vallejo, consistent with previous monitoring data for the Carquinez Strait from 2015 to 2018 at this time of year (3.47 μg/L, Schraga et al., 2018). Chlorophyll *a* was higher in Long Beach (5.42 μg/L) than in Vallejo, yet greater than the long-term average of 4.16 μg/L from 2015 to 2018 for this region during May (SCCOOS, 2019). Chlorophyll *a* in Lahaina was very low (0.03 μg/L), which was far below the 2015–2018 average of 0.27 μg/L this time of year (NOAA, 2018). By the time the ship returned to its home port of Vallejo, Chl *a* concentrations had declined by 2-fold from their early spring concentrations to 1.16 μg/L, which is lower than the 2015–2018 June average (3.08 μg/L; Schraga et al., 2018).

3.3. Microalgal cellular abundance

Benthic algal cellular abundance in the scrapings from the ship's hull (reported as cells/m^2) demonstrated the following changes from port to port (Table 2; Table 3):

Average cellular abundance declined 62% from Vallejo to sampling in Long Beach. This reduction in cellular abundance of ~194,000 cells/m^2 occurred as the ship left the low salinity waters of the SFBE and travelled in the higher salinity waters along California's coast, although temperature was similar (Table 2; Fig. 4).

Microalgal cellular abundance decreased in Lahaina, where temperature increased substantially from Long Beach: on average there was a 26% reduction across all areas of the ship resulting in an average loss of ~44,000 cells/m^2.

Cellular abundance values did not recover following the vessel's return to Vallejo (final); rather, cellular abundance remained fairly stable once the ship reached the temperate, but much less saline waters of the estuary.

A large outlier of high cellular abundance was measured at the forward section of the ship at the beginning of the voyage in Vallejo, CA, and may have obscured trends in abundance across locations on the ship. However, an additional analysis was run without this outlier which

Fig. 2. Images of typical hull fouling communities on the hull of the Training Ship *Golden Bear* taken at three locations: Vallejo, CA (initial), Lahaina, HI and Vallejo (after 2 months at sea) following the summer cruise. Variation in the ROV sampling environment is evident, especially differences in turbidity that affect visibility. Live barnacles are visible in the top and center photos, but only shells (dead barnacles) remained at the end of the voyage (bottom photo).

revealed that cellular abundance still did not differ significantly across sampling locations on the hull.

3.4. Algal photosynthetic efficiency

Algal photosynthetic efficiency, measured as *in vivo* cellular fluorescence capacity (F_v/F_m values), is generally found in the range of 0.55–0.70 in photosynthetically-efficient "healthy" marine phytoplankton (eg, Quigg et al., 2006). One area of the ship's hull had consistently lower F_v/F_m values: a nested model (lm ($F_v/F_m \sim$ Location on Hull) revealed that the aft section of the ship had significantly lower F_v/F_m values compared to the mid-ship and forward areas ($t = -0.55$, $p = 0.004$; Table 4.) Port-to-port comparisons of photosynthetic efficiency employed the average hull values of F_v/F_m from the three sampling regions on the ship's hull (Table 2, Fig. 4). Although there were no statistically significant differences, several trends were evident:

The ratio, F_v/F_m increased from Vallejo to Long Beach as the community experienced the 3-fold increase in salinity. Low F_v/F_m values in Vallejo (initial) indicated relatively photosynthetically inefficient communities (mean = 0.47 ± 0.03). F_v/F_m increased by 13% from Vallejo to Long Beach (mean = 0.54 ± 0.04).

As the vessel reached Lahaina, salinity increased modestly by 1.5, whereas temperature increased by 9.5C degrees, with a resulting 17% decline in F_v/F_m. The mean F_v/F_m. of 0.45 ± 0.26 was well below the "healthy" range typical for pelagic microalgae, and demonstrated high variability as a function of hull location.

Upon return to Vallejo, F_v/F_m values increased to the "healthy" range (mean = 0.60 ± 0.07) with the substantive declines in both salinity and temperature.

Measurements of F_v/F_m for benthic organisms (described above) followed the same trend of increasing and decreasing observed in adjacent pelagic water samples.

3.5. Microalgal biomass

Chlorophyll *a* samples collected from the three locations on the hull (forward, mid-ship, and aft) demonstrated considerable variability relative to location on the hull, but with no distinct trend:

Biomass decreased from Vallejo to Long Beach as the community experienced a 3-fold increase in salinity. There was a 42% reduction in biomass from the first initial sampling in Vallejo (mean = 6.97 ± 4.17 $\mu g/m^2$) to one week later when the vessel reached Long Beach (4.05 ± 1.91 $\mu g/m^2$), although this reduction was not statistically significant ($t = -1.00$, $p = 0.33$, Table 5).

Biomass decreased a (non-significant) further 36% from Long Beach to Lahaina, HI (mea*n* = 3.07 ± 1.29 $\mu g/m^2$) as the community experienced an extreme increase in temperature (9.5C degrees) and a modest increase in salinity from 33.5 to 35.0.

Biomass increased 230% after leaving Hawaii to a mean of 10.13 ± 8.13 $\mu g/m^2$ in Vallejo where both salinity and temperature were substantively reduced from mid-oceanic values (though not statistically significant).

3.6. Microalgal species

Navicula spp. was the dominant, and in most cases, the only observable diatom genus found on the hull samples, and was observed at every location (Fig. 3). Smaller pennate diatoms and fungi were also present at Lahaina, HI, but could not be further identified. The fungi were only observed from the forward section of the ship's hull while in Lahaina, HI. Species of *Surirella* and *Cyclotella* were present in hull samples from Long Beach, though the presence of these genera was not noted in any other samples or port locations. Overall *Navicula* was consistently observed, and the diversity of the fouling community did not appear to increase or decrease; rather, only the sporadic presence of smaller diatoms and fungi was noted throughout the voyage.

Table 2
Average algal cellular abundance, biomass (as Chl *a*), and photosynthetic efficiency (as *in vivo* cellular fluorescence capacity; F_v/F_m) for the sampling locations on the ship's hull at each port. Hull location values are the mean of triplicate (n = 3) samples ± 1 SD, when available. Ship averages are reported as means of all nine (n = 9) samples ±1 SD, when available. ND indicates no data available.

Port	Ship sample location	Cellular abundance ($\times10^3$ cells/m^2)	Ship's hull average	Cell biomass (μg/m^2)	Ship's hull average	Algal photosynthetic efficiency (F_v/F_m)	Ship's hull average
Vallejo, CA (Initial)	Forward	745.62[a]		3.50[a]		0.48[a]	
April 24, 2018	Mid-Ship	116.06 ± 65.18	314.86 ± 373.42	9.40 ± 3.56	6.97 ± 4.17	0.50 ± 0.01	0.47 ± 0.03
	Aft	89.90 ± 30.57		8.00 ± 3.50		0.44 ± 0.03	
Long Beach, CA	Forward	131.10 ± 113.19		5.40 ± 0.87		0.51 ± 0.01	
May 1, 2018	Mid-Ship	111.45 ± 88.90	121.28 ± 13.89	2.70 ± 2.25	4.05 ± 1.91	0.56 ± 0.05	0.54 ± 0.04
	Aft	ND		ND		ND	
Lahaina, HI	Forward	6.65 ± 9.01		4.50 ± 3.29		0.67 ± 0.06	
June 14. 2018	Mid-Ship	58.50 ± 50.42	57.52 ± 50.51	2.70 ± 4.02	3.07 ± 1.29	0.51 ± 0.09	0.45 ± 0.26
	Aft	107.53 ± 78.60		2.00 ± 4.00		0.16 ± 0.39	
Vallejo, CA (Final)	Forward	15.62 ± 9.92		3.50 ± 0.92		0.65 ± 0.08	
June 29, 2018	Mid-Ship	127.86 ± 119.21	58.40 ± 60.74	19.90 ± 6.60	10.13 ± 8.13	0.62 ± 0.08	0.60 ± 0.07
	Aft	32.08 ± 3.06		7.00 ± 2.15		0.52 ± 0.04	

[a] Triplicate samples not collected, only singular samples.

Table 3
Best fit model for algal cellular abundance. (A) AIC was used to select the best fit model among a model containing all variables, and nested models which remove one of the two variables: port and location on ship. dAIC is the difference in AIC of a given model from the best fit model. (B) Results of negative binomial GLM with log link function (glm.nb function, MASS package) fit to algal cellular abundance. The forward area of the ship at Vallejo (initial) is used as a baseline for comparison. *P*-values ≤ 0.05 are in bold. NA = not sampled.

A.	dAIC	df	Weight	Resid. Dev
1 Full Model	0	11	0.765	31.4
2 Without Port	3.2	4	0.158	33.2
3 Without Location on Ship	4.6	5	0.077	33.1

B.	Coefficients	Estimate	Std. Error	z value	Pr(>|z|)
Algal cellular abundance	Full Model: glm.nb(Count ~ Port * Location on Ship) AIC = 687.38				
Vallejo (Initial)	Forward	10.58	0.88	12.05	**<2e-16**
	Mid-Ship	1.08	1.08	1	0.32
	Aft	0.74	0.72	1.04	0.3
Long Beach	Forward	1.2	1.01	1.18	0.24
	Mid-Ship	−1.24	1.34	−0.93	0.35
	Aft	NA	NA	NA	NA
Lahaina	Forward	−1.8	1.01	−1.77	0.08
	Mid-Ship	1.12	1.29	0.86	0.39
	Aft	2.06	1.01	2.03	**0.04**
Vallejo (Final)	Forward	−0.95	0.72	−1.32	0.19
	Mid-Ship	1.05	1.08	0.97	0.33
	Aft	NA	NA	NA	NA
Without Port	glm.nb(Count ~ Location on Ship), AIC = 690.55				
	Forward	10.84	0.37	29.16	<2e-16
	Mid-Ship	0.69	0.51	1.34	0.18
	Aft	0.38	0.53	0.71	0.48
Without Location on Ship	glm.nb(Count ~ Port), AIC = 691.97				
	Vallejo (Initial)	11.47	0.49	23.19	<2e-16
	Long Beach	0.25	0.7	0.36	0.72
	Lahaina	−0.51	0.62	−0.83	0.41
	Vallejo (Final)	−0.5	0.62	−0.81	0.42

Table 4
Best fit model for algal photosynthetic efficiency. (A) AIC was used to select the best fit model (lower score is better) among a model containing all variables, and nested models which remove one of the two variables: port and location on ship. dAIC is the difference in AIC of a given model from the best fit model. (B) Results of a linear model fit to photosynthetic efficiency as a function of all coefficients combined. The forward area of the ship at Vallejo (initial) is used as a baseline for comparison. *P*-values ≤0.05 are in bold. NA = not sampled.

A.	dAIC	df	Weight
1 Full Model	0.7	12	0.405
2 Without Port	0	4	0.578
3 Without Location on Ship	7.1	5	0.016

B.	Coefficients	Estimate	Std. error	Pr(>|t|)
Photosynthetic efficiency	Full Model: lm(F_vF_m ~ Port * Location on Ship) AIC = −21.54			
Vallejo (Initial)	Forward	0.48	0.12	**0**
	Mid-Ship	0.02	0.14	0.86
	Aft	−0.04	0.13	0.77
Long Beach	Forward	0.04	0.13	0.78
	Mid-Ship	0.02	0.18	0.91
	Aft	NA	NA	NA
Lahaina	Forward	0.19	0.13	0.17
	Mid-Ship	−0.18	0.17	0.31
	Aft	−0.33	0.16	0.06
Vallejo (Final)	Forward	0.18	0.13	0.20
	Mid-Ship	−0.05	0.17	0.79
	Aft	−0.09	0.16	0.59
Without port	lm(F_vF_m ~ Location on Ship) AIC = −19.28			
	Forward	0.6	0.04	**0**
	Mid-Ship	−0.04	0.06	0.45
	Aft	−0.18	0.06	0
Without location on ship	lm(F_vF_m ~ Port) AIC = −11.77			
	Vallejo (Initial)	0.46	0.06	**0**
	Long Beach	0.07	0.08	0.43
	Lahaina	0.03	0.07	0.71
	Vallejo (Final)	0.14	0.07	0.07

Table 5
Best fit model for algal biomass. (A) AIC was used to select the best fit model (lower score is better) among a model containing all variables, and nested models which remove one of the two variables: port and location on ship. dAIC is the difference in AIC of a given model from the best fit model. (B) Results of a linear model fit to biomass as a function of all coefficients combined. The forward area of the ship at Vallejo (initial) is used as a baseline for comparison. *P*-values ≤0.05 are in bold. NA = not sampled.

A.	dAIC	df	Weight	Resid. Dev
1 Full Model	0	12	1	227.6
2 Without Port	21.8	4	<0.001	838.7
3 Without Location on Ship	19.5	5	<0.001	723.7

B.	Coefficients	Estimate	Std. error	t value	Pr(>|t|)
Biomass	Full Model: lm(Biomass ~ Port * Location on Ship) AIC = 166.05				
Vallejo (Initial)	Forward	3.53	3.55	0.99	0.33
	Mid-Ship	5.88	4.35	1.35	0.19
	Aft	4.16	4.1	1.01	0.32
Long Beach	Forward	1.87	4.1	0.45	0.65
	Mid-Ship	−8.62	5.43	−1.58	0.12
	Aft	NA	NA	NA	NA
Lahaina	Forward	0.98	4.1	0.23	0.81
	Mid-Ship	−7.73	5.23	−1.47	0.15
	Aft	−6.26	5.02	−1.24	0.22
Vallejo (Final)	Forward	−0.03	4.1	−0.01	0.99
	Mid-Ship	10.53	5.23	2.01	**0.05**
	Aft	−1.03	5.02	−0.2	0.83
Without Port	lm(Biomass ~ Location on Ship) AIC = 187.87				
	Forward	4.38	1.8	2.44	**0.02**
	Mid-Ship	4.81	2.54	1.9	0.07
	Aft	1.2	2.61	0.46	0.65
Without Location on Ship	lm(Biomass ~ Port) AIC = 185.43				
	Vallejo (Initial)	7.58	2.2	3.45	**0**
	Long Beach	−3.27	3.26	−1	0.33
	Lahaina	−4.38	2.84	−1.54	0.14
	Vallejo (Final)	2.44	2.84	0.86	0.4

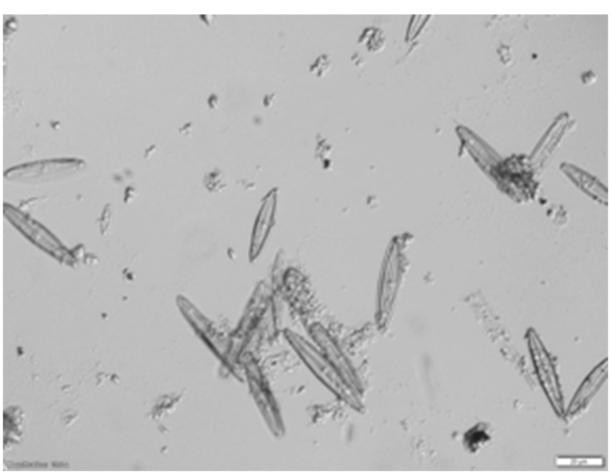

Fig. 3. Benthic microalgae collected from hull scrapings of the T.S. *Golden Bear* at Vallejo (initial sampling) on May 24, 2018 showing diatoms of the genus *Navicula*. Smaller pennate diatoms were present in lower densities, but could not be identified.

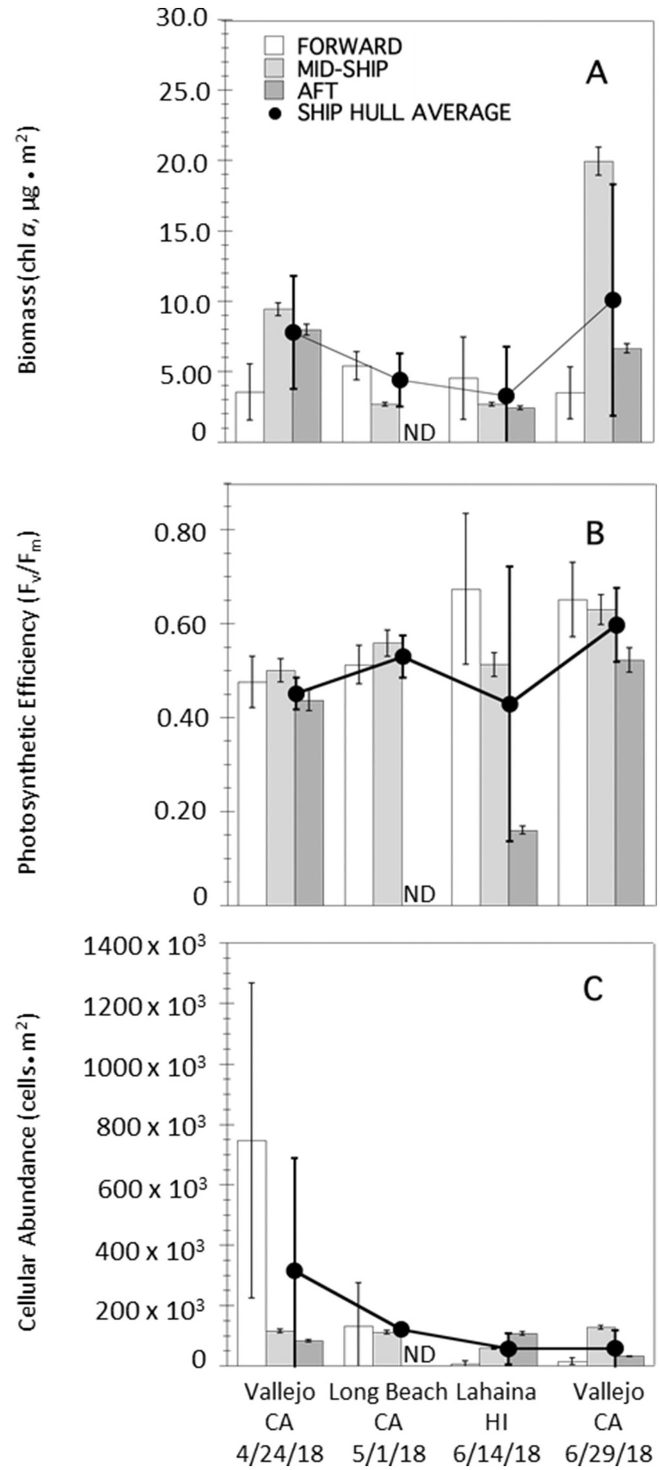

Fig. 4. (A) Algal biomass, (B) algal photosynthetic efficiency, measured as *in vivo* cellular fluorescence capacity (F_v/F_m) and (C) algal cellular abundance measured during the 2018 summer voyage of the T.S. *Golden Bear*. Shaded histograms represent averages (n = 3) samples taken from the three sections of the hull. Error bars represent ±1 SD; black jointed dots are the average of all hull measurements and are reported as the average (n = 9) ± 1 SD when available (see Table 2 for details). ND indicates no data available.

4. Discussion

4.1. Impacts of environmental conditions: macrofouling and microalgal communities

Our results suggests that portions of the microalgal community may be highly resistant to major environmental shifts that are not tolerated by macrofouling organisms. The micro- and macrofouling communities diverged sharply in their observed responses to transit. The microalgal community experienced declines in algal biomass and photosynthetic efficiency during transit, followed by recovery upon return to the estuary. Microalgal cellular abundance, however, also declined during the journey, but did not experience the same recovery.

To better evaluate the marine bioinvasion risk associated with fouling on the hulls of ships, a better understanding of the relationship between microfouling organisms and voyage characteristics, such as duration of port stays or hull husbandry practices, is necessary. At present, microfouling on in-service vessels is understudied, and while there is an abundance of macrofouling studies, it is unclear how well macrofouling responses to major shifts in environmental conditions might predict the responses of microfouling communities.

The large die-off of the macrofouling community on the T.S. *Golden Bear* aligns with previous observations of significant mortality in macrofouling communities after transiting widely variable environmental conditions, including major shifts in temperature and salinity. For example, macrofouling communities were greatly reduced on obsolete ships towed from San Francisco, CA to Brownsville, TX *via* the tropical, freshwater Panama Canal, with a massive loss in branching species, an increase in bare space, and an increase in dead barnacles and other encrusting species by the end of the voyage (Davidson et al., 2008). Reductions in macrofouling also were observed on the hulls of Canadian military ships traveling from temperate to Arctic brackish water conditions (Chan et al., 2016).

Major changes in both temperature and salinity have been shown to drive high mortality events in benthic invertebrate communities more generally. For instance, marine heat waves have caused mass mortality in a number of benthic invertebrate communities (Garrabou et al. 2009). For salinity changes, Chang et al. (2018) demonstrated how major freshwater events can result in compositional change and mass mortality in benthic macroinvertebrate communities within the SFBE. This sensitivity of estuarine and marine macrofouling communities to freshwater has led to the suggestion that flushing with freshwater could be used as a possible non-toxic means of eliminating macrofouling in semi-enclosed sea chests (Castro et al. 2018).

During transit, and at high speeds, significant shear stress imposed on the epibenthic communities on ship hulls can pull off large amounts of pre-existing growth (Davidson et al., 2020; Carlton and Hodder, 1995). We can presume that such forces are likely more important for macrofouling than microfouling organisms due to the greater surface area and thus higher drag force exerted on macrofouling organisms. Additionally, previous research has shown the resilience of diatom species such as *Navicula* to shear stress (Callow, 1986; Woods et al., 1986; Cassé and Swain, 2006; Hunsucker et al., 2014; Zargiel and Swain, 2014). Hunsucker et al. (2014) demonstrated that both *Amphora* and *Navicula* were both present in biofilms, despite combined hydrodynamic and osmotic stresses applied to mimic open-hull transport. Their results align with the continued presence of *Navicula* noted throughout the summer 2018 voyage in the present study, and may explain why the microalgal community was more resilient over the course of the journey. As noted in Hunsucker et al. (2014), these surviving microorganisms will continue to aid in further biofilm development and increase invasion risk upon macrofouling recruitment.

4.2. Biomass & algal cellular abundance

There are few published studies that focus on in-service ships and the impacts of abiotic factors and transit on microalgal species, such as diatoms (Callow, 1986; Woods et al., 1986; Zargiel et al., 2011; Hunsucker et al., 2014; Sweat et al., 2017). The present research appears to be the first to quantify the changes in microalgal communities attached to an atypically-operating vessel throughout the duration of its journey. Diatoms, the dominant members of the T.S. *Golden Bear's* microfouling community, as well as other non-cruise microfouling studies (eg, Zargiel et al., 2011) can be negatively impacted by extreme changes in environmental conditions (*i.e.*, salinity, temperature, irradiance) despite the presence of an extracellular polymeric substance, which presumably offers protection to diatoms from such stressors (Kirst, 1990; Kamer and Fong, 2001; Steele et al., 2014). Major changes in salinity (both increases and decreases) are well-known to have lethal effects on photoautotrophs, including increased osmotic and ionic stress in cells (Kirst, 1990; Kamer and Fong, 2001) and although some microalgal organisms can regulate their internal osmotic balance, it can be inferred that rapid changes in salinity resulting from resumed vessel transit could result in energetically expensive physiological changes to microalgae. Oxidative stress (Rijstenbil, 2005) and disruption of growth and photosynthetic processes (Sudhir and Murthy, 2004) have been documented as well; however, benthic diatoms embedded within a biofilm may possess a greater ability to withstand, or recover from stress stemming from high salinity exposure (Steele et al., 2014). For example, Wulff et al. (2015) demonstrated that Arctic benthic pennate diatoms are resistant to declines in salinity (from 33 to 21) over an 11-day period, finding no effects on algal cellular abundance, species composition, or photosynthetic efficiency measured with variable fluorescence. However, more extreme salinities (ie, 5 and 0) were found to have a significant deleterious effect on microalgal communities, particularly species such as *Cylindotheca closterium* (Wulff et al., 2015).

Increases in temperature can increase the cellular abundance of benthic microalgae (Admiraal, 1977) and within benthic biofilms (Russell et al., 2013), though the effects of salinity changes on such communities are not well known. The greatest declines in biomass and cellular abundance during the TS *Golden Bear*'s voyage occurred when the ship reached the high-temperature, high-saline waters of Lahaina, HI, which broadly agrees with the laboratory results of Admiraal (1977). In their laboratory study, the growth of *Navicula* sp. was examined at a range of temperatures from 4 to 25 °C, and was found to have an optimum growth temperature of ~18 °C, with growth inhibition at temperatures exceeding 20 °C. While it was suggested that *Navicula* spp. can actually utilize high temperatures (25–30 °C) during the day, this species requires lower temperatures at night to complete a high rate of cell division. These results would suggest that in the present study, the high temperatures encountered by the T.S. *Golden Bear* in Hawaii waters may have inhibited *Navicula* spp. growth and the resulting cell yield in these tropical waters.

In addition to potential stress from elevated salinity and temperature, increased irradiance in Hawaii may have negatively impacted cellular abundance and biomass. On the day of sampling in Hawaii, photosynthetically active radiation (PAR: ~400–700 nm) measured at a near-by monitoring station (Mauna Loa, Waimea, HI) was 2200 μmol photons·m^{-2}·s^{-1} (Bigelow et al., 1998). Previous research has shown that benthic diatoms often prefer low light conditions, and stress from high irradiance results in increased photoinhibition (eg, Cartaxana et al., 2013). Benthic diatoms have developed mechanisms in order to mitigate damage from high light levels: intertidal microphytobenthos have the ability to migrate downwards and avoid photoinhibition (Kromkamp et al., 1998), whereas diatoms attached to a ship may be limited by the available vertical surface on the hull. Thus, upon returning to the temperate, more turbid waters in Vallejo, CA, lower *in situ* light could have contributed to the recovery in microalgal biomass, which was composed primarily of benthic diatoms.

4.3. Algal photosynthetic efficiency

Although photosynthetic efficiency, as measured using *in vivo* cellular fluorescence capacity (F_v/F_m), did not differ significantly throughout the 2018 voyage of the T.S. *Golden Bear*, there was a non-significant decline in photosynthetic efficiency of the benthic microalgal community upon the ship's arrival in Hawaii. Physical observations of the microfouling community during sampling also suggested that the community was in poor health, as the biofilm had hardened and was difficult to pull away from the hull of the ship. Despite this decline in Hawaii, the community's cellular fluorescence capacity (F_v/F_m) values increased once the ship returned to Vallejo, CA, at the end of the voyage. Previous studies have indicated that salinity stress can have a significant impact on the maximal photochemical efficiency of photosystem II (PSII) for pelagic diatoms (Liang et al., 2014; Lu and Vonshak, 2002). Liang et al. (2014) showed that F_v/F_m decreased when *Phaeodactylum tricornutum* and *Chaetoceros gracilis* were exposed at extremely high and low salinities. Given that the microalgal community attached to the hull of the T.S. *Golden Bear* experienced an increase in salinity of 23.5 during transit from Vallejo, CA to Lahaina, HI, it seems likely that salinity stress contributed to their reduced photosynthetic efficiency.

4.4. Flow cytometry

Two methods for quantifying microalgal cellular abundance within a biofilm matrix were compared in the present study – direct counts using phase contrast microscopy and enumeration with flow cytometry. Microscopy is the traditional technique for measuring cellular abundance, and has been used successfully for decades (eg, Lund et al., 1958; Utermöhl, 1958). Cellular abundance in the present study, however, was reported based on flow cytometric estimates due to the time-intensive nature of microscopic counting and especially the difficulty in visually separating diatom cells completely from the biofilm matrix. Limited testing showed that abundance estimates from the two enumeration methods were proportional to one another. Flow cytometric results, calibrated with direct microscopic counts, were thus able to provide a rapid estimate of quantifiable changes in cellular abundance as microfouling communities were exposed to different salinities. We recommend this approach to regulators as a rapid and cost-effective method to quantify algal cellular abundance in microfouling communities on ship hulls based on these results and those of others (eg, Peperzak et al., 2018).

4.5. Remotely Operated Vehicles (ROV's)

This work demonstrated both the practical benefits and limitations of ROVs to evaluate hull fouling communities on in-service ships. In the perfect working conditions at Lahaina, HI, ROV footage allowed for a general estimate of the level of fouling, which if applied correctly, can provide a reliable estimate of biofouling extent, composition, and invasion risk (Floerl et al., 2005; Scianni et al., 2019). While the use of ROVs is a promising approach for examination of hull fouling communities *in situ* without requiring the use of diving, several important caveats should be addressed to ensure reliable data collection. Identifying macrofouling species and quantifying species abundance with a video camera while moving along a transect proved to be exceedingly difficult. Thus, there are some serious limitations and considerations when conducting hull fouling surveys with ROVs and archived video footage, including imaging issues, survey designs, sampling methods, and replication (Cordell et al., 2009; Scianni et al., 2019).

4.6. Hand-held cameras

The need for a rapid and accurate estimate of biofouling extent may require the use of other tools, rather than ROVs. This could include using a hand-held camera with a long arm attachment, as discussed in Davidson et al. (2010), for quantifying the extent and composition of biofouling on recreational boats. The use of a GoPro Hero™ video camera in the present study provided additional video footage that would not have otherwise been visible from the ROV. Our research suggests that compared to ROV use, running transects with high-quality cameras surrounded by powerful lighting alongside the ship or from a pier, may be a quicker and easier means for regulators to obtain robust data, but without decreasing accuracy especially if (1) visibility is low, (2) tides restrict maneuvering of the ROV, and (3) regulators seek to run inspections without substantially impacting operational schedules of in-service ships.

In addition to hand-held video footage (as obtained here) our qualitative measurements could have been improved by obtaining high-resolution frames at a standardized distance from the hull surface. These alternative techniques would be useful for further research as well as for regulators conducting inspections, particularly if the frequency of vessel inspections in California increases in the near future.

4.7. Physical sampling of microfouling communities on ship hulls

No significant difference was observed in the microalgal cellular abundance or biomass as a function of location on the hull (*i.e.*, forward, mid-ship and aft regions) of the T.S. *Golden Bear*. Physical sampling from the waterline and visual observations made at three distinct regions (waterline, 1 m, 2 m) allowed us to make assumptions about the fouling community at certain depths; however, the difficulty of physical hull sampling was problematic. One side of the ship (port side for the T.S. *Golden Bear*) was often inaccessible, as would be the case for the sampling of most ships while secured alongside a wharf or pier. Additionally time constraints, such as the ship's schedule, and physical factors, such as rough currents and the inability to safely approach the vessel, often occurred. This would presumably result in reduced sampling abilities for enforcement agencies and regulators.

Preferably, samples can be filtered and/or processed immediately, and quickly analyzed on-site; however the logistics of this study prevented us from either processing samples or freezing them quickly following their collection at some of the sites, notably Long Beach, CA and Lahaina, HI. Because the methods of the present study were standardized across sampling locations, the authors do not anticipate data limitations; however, it is recommended that quicker filtration, processing and analysis be implemented for similar research in the future.

Our results support the practice of taking multiple replicate samples from several areas of the ship. The current research showed no difference between the forward, mid-ship and aft regions; however, previous research has demonstrated how stressors and their impacts on organisms may vary across hull locations in other vessels (Chan et al., 2016). Thus, it would be beneficial to quantify biomass and algal cellular abundance across multiple in-service vessels to (1) establish a minimum level of replication needed to detect changes in the community, and (2) extrapolate differences between areas of the ship hull.

5. Conclusions

The biofouling regulations recently implemented by the California State Lands Commission (Scianni et al., 2019) represent an important first legal step in reducing the risk of marine invasive species transport *via* biofouling on ship hulls. Given the invasion risk posed by hull fouling, especially on atypically-operating vessels, there is a clear regulatory need for well-defined, quantitative thresholds that can be used to assess the extent of fouling easily and quickly on vessel hulls for enforcement purposes. Despite the implementation of these regulations, there is still limited understanding of the risks posed by microalgal communities transported on ship hulls, and more research is needed to examine the changes that microalgal communities undergo while in transit.

This study clearly demonstrates that microalgal communities can be highly resilient and can survive strenuous journeys through extreme variation in abiotic conditions such as salinity and temperature: from Vallejo to Long Beach, decreases in biomass (42%) and cellular abundance (62%) were observed. The transit from southern California to Hawaii resulted in further reductions of biomass (36%), cellular abundance (26%) and photosynthetic efficiency (17%). Despite reductions noted in Lahaina, HI, a final observation of the ship's hull in Vallejo revealed that the community largely recovered during its transit eastward (biomass = 230% increase; F_v/F_m = 32% increase), although cellular abundance remained fairly stable. This overall recovery poses a potentially important invasion risk to recipient systems: relatively little is known about the *in situ* responses of macrofouling and microfouling communities to changes in environmental conditions; as such, while fouling organisms could experience stress along a voyage, we propose that organisms attached to ship hulls maintain some level of invasion risk if they can survive environmental stressors (such as salinity or temperature changes) throughout a ship's voyage.

Atypically-operational ships can serve as a vector for resilient microalgal accumulation, and thus pose an invasion threat for the introduction of non-native species to new areas. Given this invasion risk posed by hull fouling, especially on atypically-operating vessels, there is a clear regulatory need for well-defined, quantitative thresholds that can be used to evaluate hull fouling levels quickly and easily on vessels for enforcement purposes. The methods used in the current research provide efficient, time-saving procedures for analyzing microalgal (and macrofouling) communities, which can in turn aid regulators in creating such necessary thresholds for enforcement.

CRediT authorship contribution statement

Christine A. Edmiston: Conceptualization, Methodology, Validation, Investigation, Writing – original draft, Project administration, Funding acquisition, Software, Data curation, Visualization. **William P. Cochlan:** Writing – original draft, Writing – review & editing, Supervision, Resources. **Christopher E. Ikeda:** Conceptualization, Software, Methodology, Resources, Data curation. **Andrew L. Chang:** Methodology, Software, Formal analysis, Data curation, Writing – original draft, Writing – review & editing, Supervision, Resources.

Declaration of competing interest

The authors declare that they have no known competing financial interests or personal relationships that could have appeared to influence the work reported in this paper.

Acknowledgements

The authors acknowledge research and travel funding provided by Dr. Edward Carpenter (SFSU). CAE - a National Science Foundation (NSF) trainee was supported by a NSF Research Traineeship Grant (NRT) - 1633336 awarded to San Francisco State University (SFSU). We thank the California State University Maritime Academy and the officers and crew of the TS *Golden Bear* for access to their vessel, and specifically the cadets and staff who assisted in this project. We thank Chris Scianni (California State Lands Commission), MISP San Francisco, and Jules Kuo (State of Hawaii) for ROV usage and piloting, and members of both the Smithsonian Environmental Research Center and the Cochlan Ecophysiology Laboratory at the Romberg Tiburon Campus of SFSU for their assistance in conducting this research.

References

Admiraal, W., 1977. Influence of light and temperature on the growth rate of estuarine benthic diatoms in culture. Mar biol 39, 1–9.
Arar, E.J., Collins, G.B., 1997. Method 445.0: In vitro determination of chlorophyll a and pheophytin a in marine and freshwater algae by fluorescence. United States Environmental Protection Agency, Office of Research and Development, National Exposure Research Laboratory, Washington (DC, pp. 601–616.
Bigelow, D.S., Slusser, J.R., Beaubien, A.F., Gibson, J.H., 1998. The USDA ultraviolet radiation monitoring program. B. Am. Metorol. Soc. 79 (4), 601–616.
Bott, T.R., 2009. Biofouling control in cooling water. Int. J. Chem. Eng. 29, 1–4.
Brandt, M.J., Johnson, K.M., Elphinston, A.J., Ratnayaka, D.D., 2009. Twort's water supply. Butterworth-Heinemann, Oxford (UK), pp. 216–217.
Burnham, K.P., Anderson, D.R., 2004. Multimodel inference: understanding AIC and BIC in model selection. Sociol. Methods Res. 33 (2), 261–304.
Callow, M.E., 1986. A world-wide survey of slime formation on anti-fouling paints. In: Evans, L.V., Hoagland, K.D. (Eds.), Algal Biofouling. Elsevier, New York (NY), pp. 1–20.
Cao, S., Wang, J., Chen, H., Chen, D., 2010. Progress of marine biofouling and antifouling technologies. Chin. Sci. Bull. 56, 598–612.
Carlton, J.T., Hodder, J., 1995. Biogeography and dispersal of coastal marine organisms: experimental studies on a replica of a 16th-century sailing vessel. Mar. Biol. 121, 721–730.
Cartaxana, P., Domingues, N., Cruz, S., Jesus, B., Laviale, M., Serôdio, J., da Silva, J.M., 2013. Photoinhibition in benthic diatom assemblages under light stress. Aquat. Microb. Ecol. 70, 87–92.
Cassé, F., Swain, G.W., 2006. The development of microfouling on four commercial antifouling coatings under static and dynamic immersion. Int. Biodeterior. Biodegradation 57, 179–185.
Castro, M.C.T.D., Vance, T., Yunnie, A.L., Fileman, T.W., Hall-Spencer, J.M., 2018. Low salinity as a biosecurity tool for minimizing biofouling on ship sea chests. Ocean Sci 14 (4), 661–667.
Chan, F.T., MacIsaac, H.J., Bailey, S.A., 2016. Survival of ship biofouling assemblages during and after voyages to the Canadian Arctic. Mar. Biol. 163, 250.
Chang, A.L., Brown, C.W., Crooks, J.A., Ruiz, G.M., 2018. Dry and wet periods drive rapid shifts in community assembly in an estuarine ecosystem. Glob. Chang. Biol. 24, 627–642.
Cordell, J., Sosik, E., Falkner, M., Scianni, C., 2009. Characterizing Risk Associated with Vessel Fouling and Non-indigenous Species in Prince William Sound. In: Prepared for the Prince William Sound Regional Citizens Advisory Council., p. 53.
Coutts, A.D., Piola, R.F., Taylor, M.D., Hewitt, C.L., Gardner, P.A., 2010. The effect of vessel speed on the survivorship of biofouling organisms at different hull locations. Biofouling. 26, 539–553.
Davidson, I.C., McCann, L.D., Fofonoff, P.W., Sytsma, M.D., Ruiz, G.M., 2008. The potential for hull-mediated species transfers by obsolete ships on their final voyages. Divers. Distrib. 14, 518–529.
Davidson, I., Sytsma, M., Ruiz, G., 2009. Ship Fouling: A Review of an Enduring Worldwide Vector of Nonindigenous Species. Aquatic Bioinvasions Research and Policy Institute Prepared for the California State Lands Commission, Marine Invasive Species Program. (111 pp).
Davidson, I.C., Zabin, C.J., Chang, A.L., Brown, C.W., Sytsma, M.D., Ruiz, G.M., 2010. Recreational boats as potential vectors of marine organisms at an invasion hotspot. Aquat. Biol. 11, 179–191.
Davidson, I., Scianni, C., Ceballos, L., Zabin, C., Ashton, G., Ruiz, G., 2014. Evaluating Ship Biofouling and Emerging Management Tools for Reducing Biofouling-mediated Species Incursions. Report to the Marine Invasive Species Program of the California State Lands Commission, Sacramento (CA) (36 pp).
Davidson, I.C., Scianni, C., Minton, M.S., Ruiz, G.M., 2017. A history of ship specialization and consequences for marine invasions, management and policy. J. Appl. Ecol. 55, 1799–1811.
Davidson, I.C., Smith, G., Ashton, G.V., Ruiz, G.M., Scianni, C., 2020. An experimental test of stationary lay-up periods and simulated transit on biofouling accumulation and transfer on ships. Biofouling. 28, 1–2.
Diatom Project. 2010. Diatoms. Part 2: Preparation of permanent slide [video]. Tokyo (JP): Mayama lab at Tokyo Gakugei University. 1 video: 6 min. https://www.youtube.com/watch?v=l-uN2RPvDSM.
Floerl, O., Inglis, G.J., Hayden, B.J., 2005. A risk-based predictive tool to prevent accidental introductions of nonindigenous marine species. Environ. Manag. 35, 765–778.
Garrabou, J., Coma, R., Bensoussan, N., Bally, M., Chevaldonné, P., Cigliano, M., Díaz, D., Harmelin, J.G., Gambi, M.C., Kersting, D.K., Ledoux, J.B., 2009. Mass mortality in Northwestern Mediterranean rocky benthic communities: effects of the 2003 heat wave. Glob. Chang. Biol 15 (5), 1090–1103.
Gollasch, S., 2002. The importance of ship hull fouling as a vector of species introductions into the North Sea. Biofouling. 18, 105–121.
Hauer, F.R., Lamberti, G.A., 2007. Section C: Stream BiotaHauer, F.R., Lamberti, G.A. (Eds.), In: Methods in stream ecology, 2nd ed. Academic Press, San Diego (CA), pp. 711–720.
Hunsucker, K.Z., Koka, A., Lund, G., Swain, G., 2014. Diatom community structure on in-service cruise ship hulls. Biofouling. 30, 1133–1140.
Ikeda, C.E., Cochlan, W.P., Bronicheski, C.M., Trainer, V.L., Trick, C.G., 2016. The effects of salinity on the cellular permeability and cytotoxicity of *Heterosigma akashiwo*. J. Phycol. 52, 745–760.
Inglis, G.J., Floerl, O., Unwin, M., Ponder-Sutton, A., Seaward, K., Kospartov, M., Bell, A., Kluza, D., 2010. The Biosecurity Risks Associated with Biofouling on International Vessels Arriving in New Zealand: Summary of the Patterns and Predictors of Fouling. NIWA Client Report prepared for MAF Biosecurity New Zealand, Wellington (NZ) (182 pp).
Kamer, K., Fong, P., 2001. Nitrogen enrichment ameliorates the negative effects of reduced salinity on the green macroalga Enteromorpha intestinalis. Mar. Ecol. Prog. Ser. 218, 87–93.

Kirst, G.O., 1990. Salinity tolerance of eukaryotic marine algae. Annu. Rev. Plant Physiol. Plant Mol. Biol. 41, 21–53.

Kromkamp, J., Barranguet, C., Peene, J., 1998. Determination of microphytobenthos PSII quantum efficiency and photosynthetic activity by means of variable chlorophyll fluorescence. Mar. Ecol. Prog. Ser. 162, 45–55.

Leary, D.H., Li, R.W., Hamdan, L.J., Hervey, W.J., Lebedev, N., Wang, Z., Deschamps, J. R., Kusterbeck, A.W., Vora, G.J., 2014. Integrated metagenomic and metaproteomic analyses of marine biofilm communities. Biofouling. 30, 1211–1223.

Lewin, R., 1984. Microbial adhesion is a sticky problem. Science. 224, 375–377.

Liang, Y., Sun, M., Tian, C., Cao, C., Li, Z., 2014. Effects of salinity stress on the growth and chlorophyll fluorescence of *Phaeodactylum tricornutum* and *Chaetoceros gracilis* (Bacillariophyceae). Bot. Mar. 57, 469–476.

Lu, C., Vonshak, A., 2002. Effects of salinity stress on photosystem II function in cyanobacterial *Spirulina platensis* cells. Physiol. Plant. 114, 405–413.

Lund, J.W.G., Kipling, C., Le Cren, E.D., 1958. The inverted microscope method of estimating algal numbers and the statistical basis of estimations by counting. Hydrobiologia 11, 143–170.

NOAA Coral Reef Watch. 2018. Updated Daily. NOAA Coral Reef Watch Version 1.0 Daily 750m VIIRS Satellite Ocean Color Monitoring – Main Hawaiian Islands. College Park (MD): NOAA Coral Reef Watch. [accessed 2018 Sept 1]. https://coralreefwatch.noaa.gov/satellite/hdf/index.php.

Parkhill, J.P., Maillet, G., Cullen, J.J., 2001. Fluorescence-based maximal quantum yield for PS II as a diagnostic of nutrient stress. J. Phycol. 37, 517–529.

Parsons, T.R., Maita, Y., Lalli, C.M., 1984. A Manual of Chemical and Biological Methods for Seawater Analysis. Permagon Press, Oxford (UK) (173 pp).

Peperzak, L., Zetsche, E.M., Gollasch, S., Artigas, L.F., Bonato, S., Creach, V., de Vré, P., Dubelaar, G.B., Henneghien, J., Hess-Erga, O.K., Langelaar, R., 2018. Comparing flow cytometry and microscopy in the quantification of vital aquatic organisms in ballast water. J Mar Eng Technol. 27, 1–10.

Quigg, A., Reinfelder, J.R., Fisher, N.S., 2006. Copper uptake kinetics in diverse marine phytoplankton. Limnol. Oceanogr. 51, 893–899.

R Core Team, 2018. R: A language and environment for statistical computing. R Foundation for Statistical Computing, Vienna, Austria. URL. https://www.R-project.org/.

Rijstenbil, J.W., 2005. UV- and salinity-induced oxidative effects in the marine diatom *Cylindrotheca closterium* during simulated emersion. Mar. Biol. 147 (1), 1063–1,073.

Ruiz, G.M., Fofonoff, P.W., Steves, B., Foss, S.F., Shiba, S.N., 2011. Marine invasion history and vector analysis of California: a hotspot for western North America. Divers. Distrib. 17, 362–373.

Russell, B.D., Connell, S.D., Findlay, H.S., Tait, K., Widdicombe, S., Mieszkowska, N., 2013. Ocean acidification and rising temperatures may increase biofilm primary productivity but decrease grazer consumption. Phil Trans R Soc B. 368, 1–11.

Southern California Coastal Ocean Observing System (SCCOOS). [accessed 2019 Nov 13]. http://www.sccoos.org/data/autoss/.

Schimanski, K.B., Goldstien, S.J., Hopkins, G.A., Atalah, J., Floerl, O., 2017. Life history stage and vessel voyage profile can influence shipping-mediated propagule pressure of non-indigenous biofouling species. Biol. Invasions 19, 2,089–2,099.

Schraga, T.S., Nejad, E.S., Martin, C.A., Cloern, J.E., 2018. USGS measurements of water quality in San Francisco Bay (CA), beginning in 2016 (ver. 2.0, June 2018): U.S. Geological Survey data release. http://www.sfbay.wr.usgs.gov.

Schultz, M.P., Bendick, J.A., Holm, E.R., Hertel, W.M., 2011. Economic impact of biofouling on a naval surface ship. Biofouling. 27, 87–98.

Scianni, C., Ceballos Osuna, L., Dobroski, N., Falkner, M., Thompson, J., Nedelcheva, R., 2019. 2019 Biennial Report on the California Marine Invasive Species Program. California State Legislature, Sacramento (CA) (123 pp).

Shapiro, H.M., 2003. Practical Flow Cytometry, 4th ed. Wiley Sons, Hoboken (NJ). (736 pp).

"International Convention for the Safety of Life at Sea (SOLAS)" 2020. International Maritime Organization (IMO). http://www.imo.org/en/About/Conventions/ListOfConventions/Pages/International-Convention-for-the-Safety-of-Life-at-Sea-(SOLAS),-1974.aspx. Retrieved May 1, 2019.

Steele, D.J., Franklin, D.J., Underwood, G.J., 2014. Protection of cells from salinity stress by extracellular polymeric substances in diatom biofilms. Biofouling. 30, 987–998.

Sudhir, P., Murthy, S.D.S., 2004. Effects of salt stress on basic processes of photosynthesis. Photosynthetica. 42, 481–486.

Sweat, L.H., Swain, G.W., Hunsucker, K.Z., Johnson, K.B., 2017. Transported biofilms and their influence on subsequent macrofouling colonization. Biofouling. 33, 433–449.

Utermöhl, H., 1958. Vervollkommnung der quantitativen phytoplankton methodik. Mitt Int Vereinigung Theoretische Angew Limnol. 9, 1–38.

Van Rompay, B., 2012. Surface Treated Composites White Book. In: HOKAPRESS, pp. 243–262.

Venables, W.N., Ripley, B.D., 2002. Chapter 10, Random and mixed effects. In: Modern applied statistics with S. Springer, New York (NY, pp. 271–300.

Wahl, M., 1989. Marine epibiosis. I. Fouling and antifouling: some basic aspects. Mar Ecol Prog Ser. 58, 175–189.

Williams, S.L., Davidson, I.C., Pasari, J.R., Ashton, G.V., Carlton, J.T., Crafton, R.E., Fontana, R.E., Grosholz, E.D., Miller, A.W., Ruiz, G.M., Zabin, C.J., 2013. Managing multiple vectors for marine invasions in an increasingly connected world. BioScience. 63, 952–966.

Woods, D.C., Fletcher, R.L., Jones, E.B.G., 1986. Diatom fouling of in-service shipping with particular reference to the influence of hydrodynamic forces. In: Round, F.E. (Ed.), Proceedings of the Ninth International Diatom Symposium. Biopress, Bristol (UK), pp. 49–59.

Wulff, A., Torstensson, A., Campana, G.L., Quartino, M.L., Zacher, K., 2015. Effects of increased temperature and decreased salinity on Antarctic benthic marine diatoms, 6th. European Phycological Congress, London (UK). 23 August 2015–28 August 2015.

Zabin, C.J., Marraffini, M., Lonhart, S.I., McCann, L., Ceballos, L., King, C., Watanabe, J., Pearse, J.S., Ruiz, G.M., 2018. Non-native species colonization of highly diverse, wave swept outer coast habitats in Central California. Mar. Biol. 165, 1–18.

Zargiel, K.A., Swain, G.W., 2014. Static vs. dynamic settlement and adhesion of diatoms to ship hull coatings. Biofouling. 30, 115–129.

Zargiel, K.A., Coogan, J.S., Swain, G.W., 2011. Diatom community structure on commercially available ship hull coatings. Biofouling. 27, 955–965.